ValenceRydberg electronic states of N2: spectroscopy and spinorbit couplings

M Hochlaf, H Ndome

Valence-Rydberg electronic states of N_2: Spectroscopy and Spin-orbit couplings

M. Hochlaf [a)], H. Ndome

Université Paris-Est, Laboratoire Modélisation et Simulation Multi Echelle, MSME UMR 8208 CNRS, 5 bd Descartes, 77454 Marne-la-Vallée, France.

D. Hammoutène

Laboratoire de Thermodynamique et Modélisation Moléculaire, Faculté de Chimie, USTHB, BP32 El Alia, 16111 Bab Ezzouar, Alger, Algeria.

M. Vervloet

Synchrotron SOLEIL, L'orme des Merisiers, Saint-Aubin - BP 48 - 91192 Gif-sur-Yvette Cedex, France.

---

a) Corresponding author:

electronic mail: hochlaf@univ-mlv.fr

Phone: +33 1 60 95 73 19

Fax: +33 1 60 95 73 20

Abstract

Using an *ab initio* methodology, we compute the potential energy curves and the spin-orbit coupling integrals of the N_2 electronic states located in the 0-120000 cm^{-1} energy domaine. In our analysis, we focus mostly on those located outside the Franck-Condon region accessible from the ground state of N_2 i.e. the two strongly bound states $1^3\Sigma_g^-$ and $1^1\Gamma_g$, and the weakly bound state $2^3\Sigma_g^-$, in addition to several repulsive states. We characterize them spectroscopically and we compute their spin-orbit couplings to the close lying singlets, triplets and quintets. This work completes our knowledge on the electronic states of N_2 that may be important intermediates during N + N collisions and for the dynamics of the N_2 singlets and triplets and quintets VUV photodissociation.

I. Introduction

For energies above 85000 cm^{-1} with respect to $N_2(X^1\Sigma_g^+, v=0)$, three groups of N_2 electronic states are known and widely studied both experimentally and theoretically: namely the $^1\Sigma_u^+$, the $^1\Pi_u$ and the $^3\Pi_u$ states. Their spectroscopy, their dynamics, their mutual interaction and their perturbation by the close lying electronic states of N_2 are nicely discussed and reviewed in Refs. [1-5]. Briefly, these electronic states are accessible (favorable Franck-Condon factors) by optical transitions from the ground state (GS) of N_2 either by spin-allowed (singlet-singlet) or spin-forbidden (singlet-triplet) absorptions [6-8]. Some triplet-triplet transitions were also well analyzed [6-8]. Outside the Franck-Condon region of GS, a quintet-quintet emitting system was detected and assigned later, by the help of theoretical calculations, to the $C''^5\Pi_u \leftarrow A'^5\Sigma_g^+$ transition, which is responsible for the Herman (HIR) bands of N_2 [9-15]. Very recently, some of us have predicted a second quintet-quintet system at higher energies [16]. It was shown there that some of these quintets couple to their close lying electronic states of triplet spin-multiplicities and participate into their perturbation as noticed experimentally [16-23].

Presently, we use state-of-the-art *ab initio* methodology for the investigation of electronic states of N_2. In light of these calculations, we reanalyze the singlets and the triplets located outside the Franck-Condon region, which are not accessible directly from N_2 GS. Using these highly correlated wavefunctions we compute the spin-orbit couplings integrals between the electronic states of N_2 lying in the 75000-120000 cm^{-1} energy domain. Then, we deduce their spectroscopic parameters. Finally, we discuss the possible perturbations of the $^1\Sigma_u^+$, the $^1\Pi_u$ and the $^3\Pi_u$ systems by these electronic states and their role on the formation of N atoms after N_2 VUV photodissociation.

II. Methodology

The calculations were done using the Complete Active Space Self Consistent Field (CASSCF) [24] technique followed by the internally contracted Multi Reference Configuration Interaction (MRCI) [25-26] approach. We described the nitrogen atom by a large basis set of aug-cc-pVQZ quality, which is augmented by 3 s and 2 p diffuse Gaussian type orbitals (GTOs) [27]. In CASSCF, the active space was composed by the valence molecular orbitals (MOs) of N_2 to which we added one σ_g and one π_g MOs for better relaxation of the wavefunctions of the N_2 electronic states whose configurations differ in their σ π orbital occupations. We used an active space larger than the valence and a diffuse basis set in order to well describe any possible Rydberg character of the electronic states treated presently. It is worth noting that such treatment does not disturb the MOs, which possess strictly a valence character as discussed previously [1,2,16]. A state-averaged procedure was used where the electronic states having the same spin and space irreducible representation in the D_{2h} point group were averaged together.

In MRCI, all CASSCF CSFs were taken as reference. All electrons were correlated. We carried out our *ab initio* electronic calculations using the MOLPRO program suite [28] in the D_{2h} point group. The B_{3u} and B_{2u} and the B_{2g} and B_{3g} representations were equivalently treated. We considered hence more than 2.6×10^8 uncontracted CSFs per symmetry. See Refs. [1,2,16] for further details.

The nuclear motion problem was solved using the method of Cooley [29]. The spectroscopic constants discussed below were obtained using the derivatives at the minimum energy distances and standard perturbation theory.

III. Potential energy curves and spectroscopy

We depict in Figure 1 the full set of our CASSCF/MRCI potential energy curves vs. the internuclear distance. These potentials are given in energy with respect to the GS minimum. This figure shows the high density of electronic states located for energies greater than 85000 cm^{-1}. This high density should favor their mutual interactions and the mixings of their wavefunctions by vibronic, spin-orbit and rotational couplings. For better clarity, we present in Figure 2 the electronic states correlating to each dissociation limit separately together with their assignments. We considered electronic states that converge adiabatically to the $N(^4S_u) + N(^4S_u)$, $N(^4S_u) + N(^2D_u)$, $N(^4S_u) + N(^2P_u)$, and $N(^2D_u) + N(^2D_u)$ asymptotes. Generally, the pattern of the electronic states located in the domain of interest is in good accord with the previously ones. For instance, this is the case for the majority of the electronic states located in the Franck-Condon region so that we will not discuss them in detail. In addition, our calculations allow better description of some singlet and triplet states lying at high energies. These states are either strongly or weakly bound or repulsive in nature. In the following, we focus on the spectroscopy of the bound states and their spin-orbit interactions with the close-lying

electronic states of N_2. The repulsive states are mostly of quintet spin multiplicity. They were widely discussed and commented in Ref. [16]. It is worth noting that the literature on the N_2 electronic states is wide and it is not the scope of the present paper to enumerate it. Instead we present our results and their comparison to the earlier VCI treatment of Michels [30] and to the multi configuration interaction study of Mulliken and co-workers [31]. These two theoretical works represent the most complete treatments of the N_2 electronic states. The analysis of the electron configurations of these electronic states coincides with its performed by Mulliken and co-workers in Ref. [31]. Especially, the valence or Rydberg or mixed character of these electronic states is confirmed by the present calculations.

In the 90 x 10^3 - 120 x 10^3 cm^{-1} energy range, we calculate three bound states located outside the Franck-Condon region from GS:

(i) At ~ 97800 cm^{-1}, we locate a relatively strongly bound electronic state of $^3\Sigma_g^-$ symmetry (Figure 2C, Table 1). It possesses a potential well of ~8700 cm^{-1}. Its electronic wavefunction is mainly described by the $(2\sigma_g)^2(3\sigma_g)^2(1\pi_u)^2(2\sigma_u)^2(1\pi_g)^2$ similar to the $N_2(G^3\Delta_g)$ state and to the outer part of the $N_2(a"^1\Sigma_g^+)$ state. Formally, we add an electron into the vacant $1\pi_g$ molecular orbital to the ionic core $N_2^+(b^4\Pi_g)$ [32]. The equilibrium distance of $N_2(1^3\Sigma_g^-)$ is calculated 1.614 Å, which is close enough to the equilibrium value in $N_2^+(b^4\Pi_g)$ (1.46 Å [32]). This electronic state was previously predicted by Michels [30] in 1979. However, this prediction was strongly criticized two years later by Mulliken and co-workers [31] because of the small active space used in Michels's work. Nevertheless, our large calculations confirm the earlier predictions of Michels. At the MRCI level, we calculate ω_e $(1^3\Sigma_g^-)$ = 761 cm^{-1} which is 31 cm^{-1} smaller than the value given by Michels (Table1).

(ii) We find a $^1\Gamma_g$ state that correlates adiabatically to the $N(^2D_u)$ + $N(^2D_u)$ dissociation limit (Figure 2 D). The existence of this electronic state was already noticed by Ermler *et al.* [31]. These authors calculated the potential curve for the $1^1\Gamma_g$ state up to R=3.2 bohr (= 1.693 Å) and found in their best SD calculation a pronounced minimum at 13.14 eV (= 106000 cm^{-1}). The VCI treatment of Michels led also to a strongly bound state. Our calculations confirm definitely that this electronic state is well bound with a deep potential well of ~13750 cm^{-1}. Its electronic wavefunction is dominantly described by the $N_2^+(b^4\Pi_g) + 1\pi_g$ electron configuration. At the MRCI level of theory, we compute the following spectroscopic parameters for this electronic state: R_e = 1.608 Å, B_e = 0.9305 cm^{-1}, α_e = 0.0123 cm^{-1}, ω_e = 816.5 cm^{-1}, $\omega_e x_e$ = 9.35 cm^{-1} and $\omega_e y_e$ = -0.14 cm^{-1} (Table 1). Our R_e, B_e, α_e and $\omega_e x_e$ agree with those of Michels [30], whereas our ω_e is ~40 cm^{-1} smaller than his value.

(iii) In Michels's work, a $^3\Sigma_g^-$ state was found for energies ~ 114000 cm^{-1}. Nevertheless, the shape of the potential of this electronic state was not definitely established there because of the reduced size of his calculations. This author predicted a double well potential for this

electronic state. Our calculations confirm the presence of such electronic state but a unique shallow potential well is found. It corresponds to the $2^3\Sigma_g^-$ state at ~ 114500 cm^{-1}. The depth of the potential is ~ 2200 cm^{-1}. The $2^3\Sigma_g^-$ equilibrium distance is 1.817 Å. The formation of such shallow potential well is most likely due to competition between electrostatic interactions and the chemical bonding between two $N(^2D_u)$ atoms (Figure 2D). This electronic state is multi configurational in nature: its wavefunction is dominantly described by the $(2\sigma_g)^2(3\sigma_g)^2(1\pi_u)^2(2\sigma_u)^2(1\pi_g)^2$ and $(2\sigma_g)^2(3\sigma_g)^0(1\pi_u)^4(2\sigma_u)^2(1\pi_g)^2$ electron configurations.

Table 1 presents the spectroscopic properties of these three electronic states. We list also the data for the $a'^1\Sigma_u^-$, $a^1\Pi_g$, $w^1\Delta_u$, $G^3\Delta_g$, $a''^1\Sigma_g^+$ and $E^3\Sigma_g^+$ states, where a close comparison with the reference data of [7,33-35] is given. For the later states, one can clearly see the good accord between our calculated harmonic and anharmonic terms and rotational constants and those determined experimentally. Indeed, the calculated and measured equilibrium distances differ by less than 0.01 Å, which is connected also to the noticeable good agreement for the rotational constants at equilibrium, B_e. For the harmonic wavenumbers ($?_e$), the differences are less than 10 cm^{-1}, except for the E state where we compute a value larger than Refs. [34,35] by 29 cm^{-1} . Such good agreement asserts on the good quality of the predicted spectroscopic data for the of $N_2(1^3\Sigma_g^-, 1^1\Gamma_g$ and $2^3\Sigma_g^-)$ electronic states.

IV. Spin-orbit couplings

We evaluated the spin-orbit coupling terms between the electronic states of interest over the CASSCF wavefunctions and using the Breit-Pauli Hamiltonian as implemented in MOLPRO. These integrals are calculated in Cartesian coordinates. Figure 3 displays the non-vanishing non-diagonal spin-orbit integrals between the singlet, triplet and quintet N_2 electronic states. In this figure, we use the following notation: A-B denotes the $<A|H^{SO}|B>$ integral. For instance, the $E^3\Sigma_g^+$-$2^3\Sigma_g^-$ term corresponds to the $< E^3\Sigma_g^+|H^{SO}|2^3\Sigma_g^->$ integral. In the following, we discuss solely the spin-orbit evolutions. In particular, we do not consider their consequences on the spectroscopic parameters of the N_2 electronic states since spin-orbit corrections to the spin-orbit free PECs of Figures 1 and 2 are too small for N_2.

Figure 3 shows that the spin-orbit integrals present two different behaviours: For R < 3-3.5 bohr, they exhibit a non-monotonic evolution along the internuclear distance, whereas they are mostly monotonic or quasi constant for R > 3.5 bohr. These brusque changes coincide with the change of the nature of the corresponding electronic wavefunctions. For instance, the $E^3\Sigma_g^+$, $a''^1\Sigma_g^+$, and $^3\Pi_u$ electronic states present potential barriers separating their potential wells at short and large internuclear separations (within the adiabatic representation). This is accompanied by strong variations

of the composition of their wavefunctions, resulting in drastic changes in the spin-orbit integrals evolving these three electronic states.

Recently, we calculated the spin-orbit constants at equilibrium ($A_{SO,e}$) for the quintet and the $^3\Pi_u$ states using similar methodology. An excellent accord is found with experimental determinations [2, 16]. The present data allow deducing $A_{SO,e}$ ($G^3\Delta_g$) = ½ $<G^3\Delta_g|H^{SO}|\ G^3\Delta_g>$ = -0.04 cm^{-1}. We confirm hence the close to zero spin-orbit constants (A_0 = -0.21 and A_1 = -0.25 cm^{-1}) measured earlier for this electronic state [36].

V. Discussion

In this section, we detail the implications of the presence of the $1^3\Sigma_g^-$, $1^1\Gamma_g$ and $2^3\Sigma_g^-$ electronic states in the radiative transitions and perturbations of the well-known electronic states of N_2. Then we use our PECs and spin-orbit coupling integral evolutions to treat the interactions of these electronic states with the other electronic states.

1. Implications for the radiative transitions in N_2

In despite that the $1^3\Sigma_g^-$ state is located relatively high in energy, this state cannot emit to the lowest electronic states of N_2 due to selection rules for optical transitions. This confers a relative stability to this triplet. In contrast, it can undergo radiative transitions to the $^3\Pi_u$ states. For instance, it may interact with the neighboring $C^3\Pi_u$, $C'^3\Pi_u$, and $III^3\Pi_u$ states. For R = 3.06 bohr (~ R_e of $1^3\Sigma_g^-$), we compute the following transition moments: $<1^3\Sigma_g^-|\mu|C^3\Pi_u>$ = -0.221, $<1^3\Sigma_g^-|\mu|C'^3\Pi_u>$ = -0.123 and $<1^3\Sigma_g^-|\mu|III^3\Pi_u>$ = -0.430, in Debye. As shown in Figure 4, transitions in the IR between the low vibrational levels of both sets of triplet states are most likely occurring.

At ~ 96 x 10^3 cm^{-1} above GS, the E state was first located through the analysis of the $E^3\Sigma_g^+$? $A^3\Sigma_u^+$ emissions (Herman-Kaplan system) [37]. This assignment was definitely confirmed later theoretically and experimentally [34,35,38-41]. Our calculations show that the $1^3\Sigma_g^-$ is lying closely to the E state. The $E^3\Sigma_g^+ \rightarrow A^3\Sigma_u^+$ emission is allowed, whereas the $1^3\Sigma_g^- \rightarrow A^3\Sigma_u^+$ radiative transition is not. Accordingly, the emission spectra of N_2 near to the Herman-Kaplan bands should be perturbed by the existence of the $1^3\Sigma_g^-$ state: several observations relative to this band system remain still unexplained. For instance, Beiting and Feldman [42] found that the intensity of the (0, 2) band of the Herman-Kaplan (E ? A) system was ~5 times stronger than the previously predicted theoretical value. Moreover, the relatively long radiative lifetime for the E state of 270 ± 100 μs measured by Freund [35] is probably because of the population of the E rovibrational levels by spin-orbit conversions from the $1^3\Sigma_g^-$ acting as a reservoir for the emitting E state (see below).

The $1^1\Gamma_g$ state can decay radiatively to the lower $W^3\Delta_u$. However, this transition should be very weak because it is spin-forbidden and because |? ? | > 1. Hence, the rovibrational levels of $1^1\Gamma_g$ should have long lifetimes. Alternatively, it can be populated by optical emissions from the upper bound $^1\Delta_u$ or $^1\Gamma_u$ Rydberg states of N_2 or via spin-forbidden transitions from the upper $^3\Delta_u$ and ^3F_u (e.g. H ^3F_u).

Finally, the $2^3\Sigma_g^-$ state should play a central role during the cascading optical transitions involving the Valence-Rydberg and Rydberg states of N_2. For instance, Figure 4 shows that this triplet is embedded into a set of $^3\Pi_u$ states to which it can either emit (e.g. to the $C^3\Pi_u$ and $C'^3\Pi_u$ states) or couple (e. g. with the $III^3\Pi_u$ state) and *vice versa*. The $^3\Pi_u$ states lying above $III^3\Pi_u$, which present a non-zero Franck-Condon overlap with the $2^3\Sigma_g^-$ may be invoked in that context.

2. On the role of N_2 ($1^3S_g^-$, 1^1G_g, $2^3S_g^-$) in the dynamics of the neighboring electronic states and in N_2 VUV photodissociation

For a diatomic homonuclear molecular system, the spin-orbit interaction selection rules are [43,44]:

$\Delta\Omega = 0$; g ? /? u; g ? g; u ? u; Σ^+ ? Σ^-

$\Delta S = 0$ or $\Delta S = \pm 1$; $\Delta\Lambda = \Delta\Sigma = 0$ or $\Delta\Lambda = -\Delta\Sigma = \pm 1$

Therefore, *ungerade* states couple together and *gerade* states couple together. We have already treated in Ref. [16] the possible interactions between the *ungerade* states of N_2, where we have enlightened the role of the bound and repulsive quintet states. These quintets connect the singlets and the triplets located in the Franck Condon region of GS to the corresponding photodissociation products. Presently, we consider the interactions between the *gerade* states. We focus mostly on the role of $1^3\Sigma_g^-$, $1^1\Gamma_g$ and $2^3\Sigma_g^-$. We display in Figure 5 the PECs of these electronic states together with those of the other *gerade* states crossing them.

For $N_2(1^3\Sigma_g^-)$, the situation is rather complicated since this triplet is embedded into a set of potentials of electronic states to which *a priori* it can couple. Indeed, Figure 5 reveals that $1^3\Sigma_g^-$ is crossed by the $2^5\Sigma_g^+$, $E^3\Sigma_g^+$, a"$^1\Sigma_g^+$, $1^5\Pi_g$, $^5\Delta_g$ and $a^1\Pi_g$. Among them, only the $1^3\Sigma_g^-$? $E^3\Sigma_g^+$, $1^3\Sigma_g^-$? $1^5\Pi_g$ and $1^3\Sigma_g^-$? $a^1\Pi_g$ spin-orbit conversions are allowed. The $<1^3\Sigma_g^-|H^{SO}|a^1\Pi_g>$ integral (not shown) is close to zero along the NN distance. Whereas, the $<1^3\Sigma_g^-|H^{SO}|E^3\Sigma_g^+>$ and $<1^3\Sigma_g^-|H^{SO}|1^5\Pi_g>$ integrals amount to ~ 5.9 and ~ 25.5 (in cm^{-1}) at their crossings (i.e. R = 2.48 bohr and R = 3.93 bohr), respectively. Such integrals are large enough to allow such conversion. The $1^5\Pi_g$ is repulsive in nature. It correlates adiabatically to the $N(^2D_u)$ + $N(^4S_u)$ asymptote. It leads hence directly to the $N(^2D_u)$ + $N(^4S_u)$ products. For the E vibrational levels located above the $E^3\Sigma_g^+$ - $1^3\Sigma_g^-$ crossing, we expect the

following successive transitions: $E^3\Sigma_g^+ \rightarrow 1^3\Sigma_g^- \rightarrow 1^5\Pi_g \rightarrow N(^2D_u) + N(^4S_u)$. This reduces their lifetimes. For the lower rovibrational states, they should have, instead, long lifetimes.

The $1^1\Gamma_g$ state presents a large orbital angular momentum, Λ. It should be free from any interactions or better saying weakly coupled to the N_2 states in despite that it is crossed by the $E^3\Sigma_g^+$, $2^5\Sigma_g^+$, $1^5\Pi_g$, $^5\Delta_g$, $2^3\Pi_g$, $a^1\Pi_g$, $1^5\Pi_g$ $1^5\Sigma_g^-$ and $2^5\Pi_g$ states. According to the selection rules given above, it cannot couple to any of these states by spin-orbit. For the formation of N_2 molecules in the $1^1\Gamma_g$ state, we can propose either reactive collisions between $N^*(^2D_u)$ and $N^*(^2D_u)$ atoms or by radiative transitions from the upper $^3\Delta_u$ states of N_2.

Similar to the $1^3\Sigma_g^-$ state, the $N_2(2^3\Sigma_g^-)$ is crossed by a multitude of *gerade* states. Spin-orbit conversions may occur only with the $E^3\Sigma_g^+$, $2^3\Pi_g$, $1^5\Pi_g$ and $2^5\Pi_g$ states (Figure 5). The spin-orbit integrals are non-zero at their crossings (Figure 3). Close to and beyond the region of the crossings, the $E^3\Sigma_g^+$, $2^3\Pi_g$, $1^5\Pi_g$ and $2^5\Pi_g$ states present dissociative behaviors and lead to the lower asymptotes. The dynamics of the rovibrational levels supported by the $2^3\Sigma_g^-$ weak potential should be complex. This should affect the lifetimes of such levels. In addition, we expect that the $2^3\Sigma_g^-$ state plays crucial roles during cold collisions between two $N(^2D_u)$ atoms and in the dynamics of the Valence-Rydberg states lying in energy close to the $N(^2D_u) + N(^2D_u)$ asymptote via couplings to the triplet and quintet states.

VI. Conclusion

Using a full *ab initio* treatment, we investigated the electronic states of N_2. In addition to the well-known electronic states, we confirm the existence of three bound *gerade* states. These states possess potential wells located outside the Franck-Condon region accessible from $N_2(X^1\Sigma_g^+)$ or from the metastable $(A^3\Sigma_u^+)$ state. Experimental evidences of their existence and their interactions and perturbations of the singlet, triplet and quintet manifolds of states are discussed. Therefore, we strongly recommend the consideration of these electronic states in the analysis of the N_2 spectra at these energies even those located in the FC region. In the near future, we will be computing the non-adiabatic couplings between these electronic excited states.

This work should motivate new experimental investigations dealing with N_2, especially the *gerade* states using, for instance, multiphoton absorption techniques. We could also suggest the study of the emission spectra of electric discharges established in supersonic jets, where one may observe simultaneously N_2 emitting systems of any spin multiplicity, rotationally cold, similar to those allowed the identification of Herman's quintet system.

References

1. D. Spelsberg and W. Meyer. J. Chem. Phys. **115**, 6438 (2001).
2. H. Ndome, M. Hochlaf, B. R. Lewis, A. N. Heays, S. T. Gibson and H. Lefebvre-Brion. J. Chem. Phys. **129**, 164307 (2008).
3. B. R. Lewis, K. G. H. Baldwin, J. P. Sprengers, W. Ubachs, G. Stark and K. Yoshino. J. Chem. Phys. **129**, 164305 (2008) and references therein.
4. X. Liu, A. N. Heays, D. E. Shemansky, B. R. Lewis and P. D. Feldman. J. Geophys. Research D: Atmospheres **114**, D07304 (2009).
5. J. Bruna and F. Grein. Can. J. Phys. **87**, 589 (2009).
6. P. F. Bernath and S. McLeod, DiRef, a database of references associated with the spectra of diatomic molecules, J. Mol. Spectrosc. **207**, 287. (2001).
7. K. P. Huber and G. Herzberg, in *Molecular spectra and molecular structure Constants of diatomic molecules*, 4.van Nostrand Reinhold, New York, USA (1979).
8. A. Lofthus and P. H. Krupenie. J. Phys. Chem. Ref. Data **6**, 113(1977).
9. R. Hermann. C. R. Acad Sci. (Paris) **233**, 738 (1951).
10. H. Partridge, S. R. Langhoff, C. W. Bauschlicher, Jr. and D. W. Schwenke. J. Chem. Phys. **88**, 3174 (1988).
11. R. W. Field, O. Pirali and D. W. Tokaryk. J. Chem. Phys. **124**, 081103 (2006).
12. K. P. Huber and M. Vervloet. J. Chem. Phys. **89**, 5957 (1988).
13. K. P. Huber and M. Vervloet. J. Mol. Spectrosc. **153**, 17 (1992).
14. O. Pirali and D. W. Tokaryk. J. Chem. Phys. **124**, 081102 (2006).
15. O. Pirali and D. W. Tokaryk. J. Chem. Phys. **125**, 204308 (2006).
16. M. Hochlaf, H. Ndome and D. Hammoutène. J. Chem. Phys. **132**, 104310 (2010).
17. Ch. Ottinger and A. Vilesov. J. Chem. Phys. **100**, 4862 (1994).
18. Ch. Ottinger and A. Vilesov. J. Chem. Phys. **103**, 9929 (1995).
19. W. J. Marinelli, W. J. Kessler, A. M. Woodward and W.T. Rawlins. J. Chem. Phys. **92**, 1796 (1990).
20. J. S. Morrill and W. M. Benesch. J. Chem. Phys. **101**, 6529 (1994).
21. J. Berkowitz, W. A. Chupka and G. B. Kistiakowsky. J. Chem. Phys. **25**, 457 (1956).
22. E. E. Antonov and V. I. Popovich. Opt. Spectrosc. **67**, 172 (1989).
23. F. Roux, F. Michaud and M. Vervloet. J. Mol. Spectrosc. **158**, 270 (1993).
24. P. J. Knowles and H.-J. Werner. Chem. Phys. Lett. **115**, 259 (1985).
25. H.-J. Werner and P. J. Knowles. J. Chem. Phys. **89**, 5803 (1988).
26. P. J. Knowles and H.-J. Werner. Chem. Phys. Lett. **145**, 514 (1988).
27. T. H. Dunning Jr. J. Chem. Phys. **90**, 1007 (1989).
28. http://www.molpro.net.

29. J. W. Cooley. Math. Comput. **15**, 363 (1961).
30. H. H. Michels, in Electronic structure of excited states of selected atmospheric systems", Ed. J. W. McGowan, Advanced Chemical Physics **45**, 225 (1981).
31. W. C. Ermler, A. D. McLean and R. S. Mulliken. J. Phys. Chem. **86**, 1305 (1982).
32. M. Hochlaf, G. Chambaud and P. Rosmus. J. Phys. B **30**, 4509 (1997).
33. http://webbook.nist.gov.
34. P. K. Carroll and A. P. Doheny. J. Mol. Spectrosc. **50**, 257 (1974).
35. R. Freund. J. Chem. Phys. **50**, 3734 (1969).
36. P. K. Carroll, C. C. Collins and J. T. Murnaghan. J. Phys. B **5**, 1634 (1972).
37. R. Herman, Ann. Phys. **20**, 241 (1945).
38. L. W. Borst and E. C. Zipf. Phys. Rev. A: Gen. Phys. **3**, 979 (1971).
39. P. K. Carroll and N. D. Sayers. Proc. Phys. Soc. A **66**, 1138 (1953).
40. A. G. Gaydon and R. Herman. Proc. Phys. Soc. **58**, 292 (1946).
41. M. Zubek and G. King. J. Phys. B: At. Mol. Opt. Phys. **27** 2613 (1994).
42. J. Beiting III and P. D. Feldman. J. Geoph. Res. **84**, 1287 (1979).
43. K. Kayama and J. C. Baird. J. Chem. Phys. **46**, 2604 (1967).
44. H. Lefebvre-Brion and R.W. Field, (2004), *The Spectra and Dynamics of Diatomic Molecules*; Elsevier Academic Press: Amsterdam / Boston / Heidelberg / London / New York / Oxford / Paris / San Diego / San Francisco / Singapore / Sidney / Tokyo, 2004.
45. B. R. Lewis, A. N. Heays, S. T. Gibson, H. Lefebvre-Brion and R. Lefebvre. J. Chem. Phys. **129**, 164306 (2008).

Table1: Excitation energy (T_e, in cm^{-1}), equilibrium distance (R_e, in Å), rotational constants (B_e, α_e; in cm^{-1}), harmonic wavenumbers (ω_e, in cm^{-1}) and anharmonic terms ($\omega_e x_e$, $\omega_e y_e$, in cm^{-1}) of the valence-Rydberg states of N_2. Second entry corresponds to the data from [33]. For the quintets located at these energies, readers are referred to Ref. [16].

State		T_e	R_e	B_e	α_e	ω_e	$\omega_e x_e$	$\omega_e y_e$
$a'^1\Sigma_u^-$		69032 68152.66	1.278 1.2755	1.4725 1.4799	0.0166 0.0166	1523.6 1530.25	11.91 12.0747	0.028
$a^1\Pi_g$		69971 69283.06	1.225 1.2203	1.6034 1.6169	0.0178 0.0179	1687.5 1694.20	13.91 13.949	0.0183
$w^1\Delta_u$		73494 72097.4	1.271 1.268	1.4910 1.498	0.0160 0.0166	1559.1 1559.26	12.39 11.63	0.154
$G^3\Delta_g$		89721 87900	1.615 1.6107	0.9224 0.9280	0.0167 0.0161	749.6 742.49	11.74 11.85	-0.17
$a''^1\Sigma_g^+$	Inner well [a]	95914	1.105	1.9704	0.100			
	Outer well	90521	1.558	0.9915	0.010	933.9	-2.16	-1.40
$E^3\Sigma_g^+$		95900 95858 95747.50 [b]	1.121 1.117 1.16 [b]	1.914 1.927 1.927 [b]	0.03	2216.3 2185	12.8	-0.4
$1^3\Sigma_g^-$		97776 97109 [c]	1.614 1.61 [c]	0.9225 0.93 [c]	0.016 0.0079 [c]	761.0 792.0 [c]	12.16 7.4 [c]	-0.14
$1^1\Gamma_g$		102993 100738 [c]	1.608 1.60 [c]	0.9305 0.94 [c]	0.0123 0.011 [c]	816.5 856.2 [c]	9.35 9.7 [c]	-0.14
$2^3\Sigma_g^-$		114580	1.817	0.7285	0.015	428.0	9.27	-0.81

a) Three vibrational levels are calculated at 1637.9, 4727.1 and 8116.86 (in cm^{-1}), respectively.

b) Refs. [34,35]

c) Ref. [30]

Figure captions:

Figure 1: Overview of the MRCI potential energy curves of the electronic states of N_2 investigated presently. These curves are given in energy with respect to the ground state minimum energy.

Figure 2: Potentials of the electronic states correlating to the $N(^4S_u) + N(^4S_u)$ (in A), $N(^4S_u) + N(^2D_u)$ (in B), $N(^4S_u) + N(^2P_u)$ (in C) and $N(^2D_u) + N(^2D_u)$ (in D). These PECs can be sent upon request.

Figure 3: Evolution of the spin-orbit integrals. These curves can be sent upon request

Figure 4: PECs of the $^3\Pi_u$ and $^3\Sigma_g^-$ states. The horizontal lines correspond to the positions of some vibrational levels of $C^3\Pi_u$ as given in Ref. [45]. The *ab initio* curves are shifted down by 2090 cm^{-1} to match the experimental data for $C^3\Pi_u$.

Figure 5: Interactions of the $1^3\Sigma_g^-$, $1^1\Gamma_g$ and $2^3\Sigma_g^-$ states with the close lying states.

Figure 1

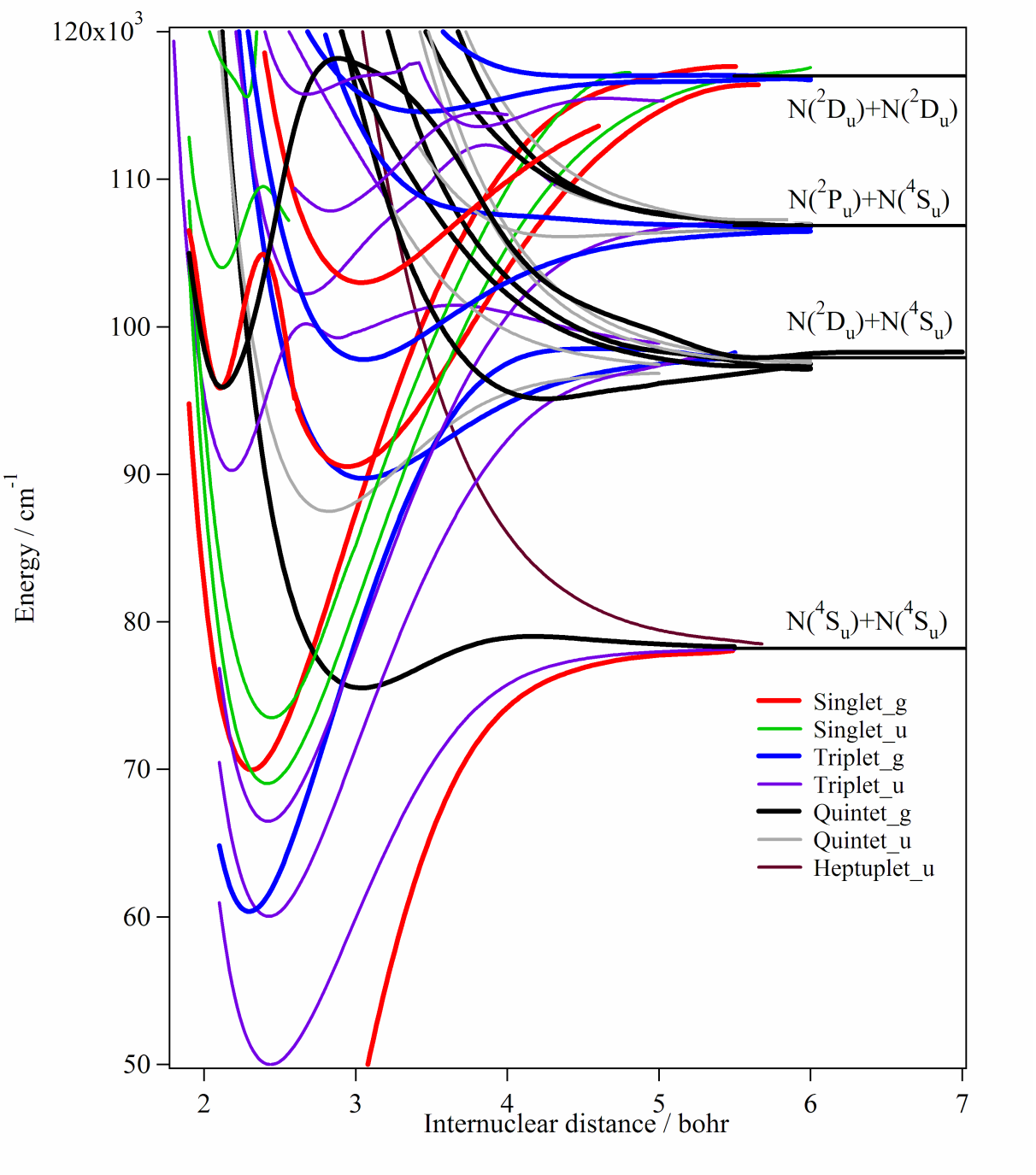
120x10^3
110
100
90
80
70
60
50
Energy / cm^-1
2
3
4
5
6
7
Internuclear distance / bohr
N(2Du)+N(2Du)
N(2Pu)+N(4Su)
N(2Du)+N(4Su)
N(4Su)+N(4Su)
Singlet_g
Singlet_u
Triplet_g
Triplet_u
Quintet_g
Quintet_u
Heptuplet_u

Figure 2

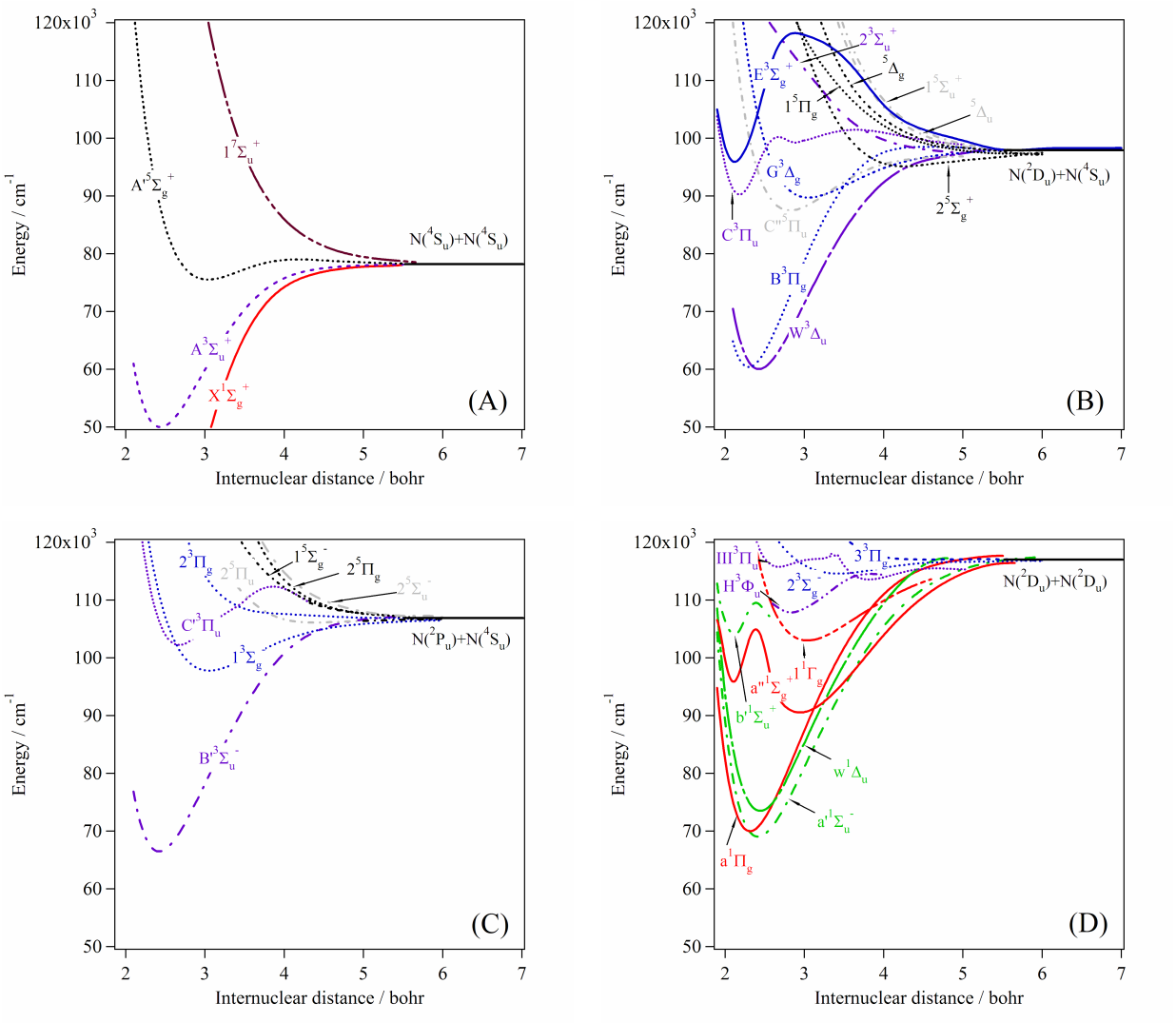
120x10^3
110
100
90
80
70
60
50
Energy / cm^-1
2
3
4
5
6
7
Internuclear distance / bohr
A''5Σg+
1 7Σu+
N(4Su)+N(4Su)
A 3Σu+
X 1Σg+
(A)
E 3Σg+
2 3Σu+
5Δg
1 5Σu+
1 5Πg
5Δu
G 3Δg
N(2Du)+N(4Su)
2 5Σg+
C 3Πu
C'' 5Πu
B 3Πg
W 3Δu
(B)
2 3Πg
2 5Πu
1 5Σg-
2 5Πg
2 5Σu-
C 3Πu
N(2Pu)+N(4Su)
1 3Σg-
B'' 3Σu-
(C)
III 3Πu
3 3Πg
H 3Φu
2 3Σg-
N(2Du)+N(2Du)
a'' 1Σg+
1 1Γg
b' 1Σu+
w 1Δu
a' 1Σu-
a 1Πg
(D)

Figure 3

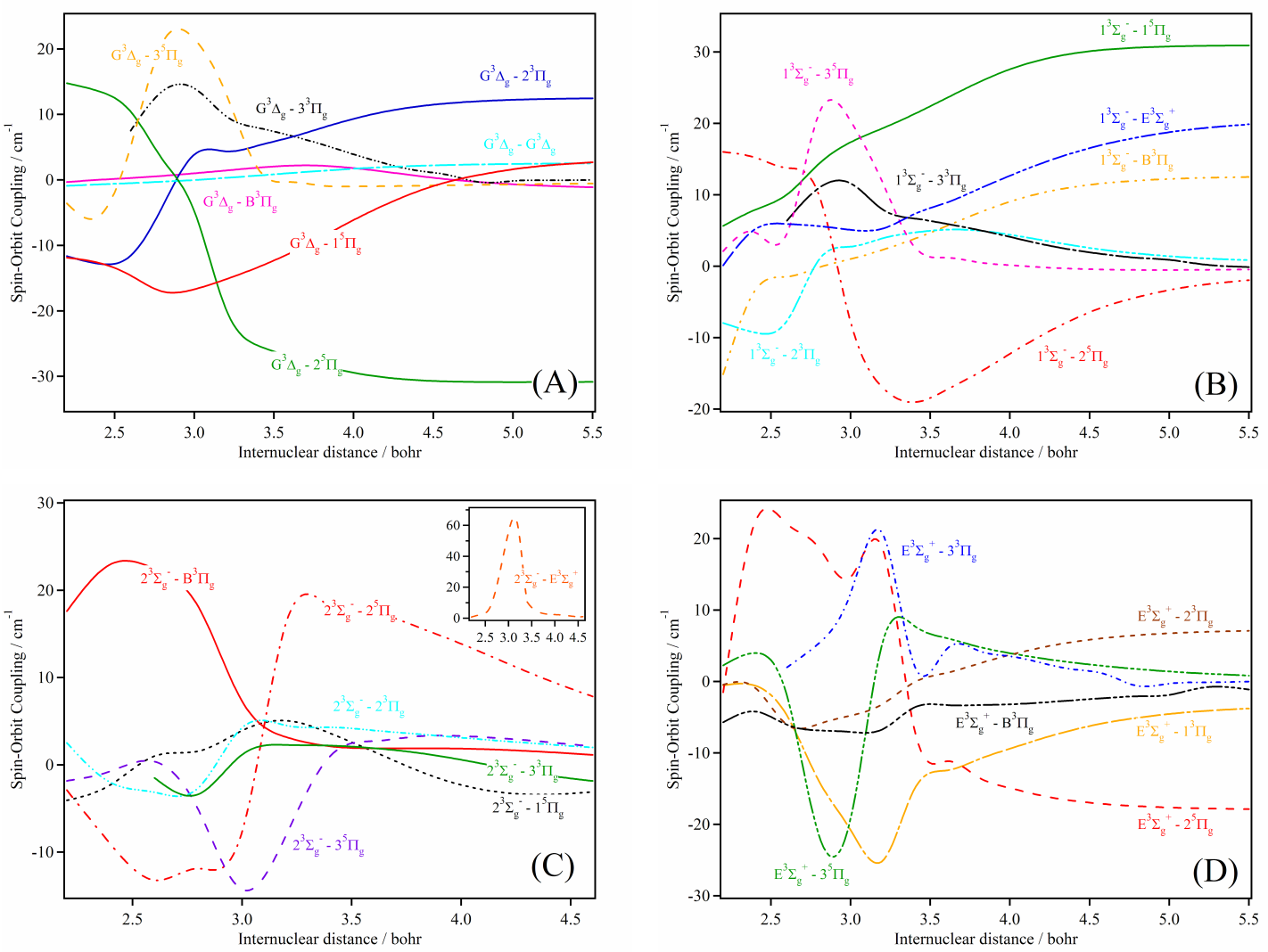
Spin-Orbit Coupling / cm^{-1}
Internuclear distance / bohr
$G^3\Delta_g$ - $3^5\Pi_g$
$G^3\Delta_g$ - $2^3\Pi_g$
$G^3\Delta_g$ - $3^3\Pi_g$
$G^3\Delta_g$ - $G^3\Delta_g$
$G^3\Delta_g$ - $B^3\Pi_g$
$G^3\Delta_g$ - $1^5\Pi_g$
$G^3\Delta_g$ - $2^5\Pi_g$
(A)
$1^3\Sigma_g^-$ - $1^5\Pi_g$
$1^3\Sigma_g^-$ - $3^5\Pi_g$
$1^3\Sigma_g^-$ - $E^3\Sigma_g^+$
$1^3\Sigma_g^-$ - $3^3\Pi_g$
$1^3\Sigma_g^-$ - $B^3\Pi_g$
$1^3\Sigma_g^-$ - $2^3\Pi_g$
$1^3\Sigma_g^-$ - $2^5\Pi_g$
(B)
$2^3\Sigma_g^-$ - $B^3\Pi_g$
$2^3\Sigma_g^-$ - $2^5\Pi_g$
$2^3\Sigma_g^-$ - $E^3\Sigma_g^+$
$2^3\Sigma_g^-$ - $2^3\Pi_g$
$2^3\Sigma_g^-$ - $3^3\Pi_g$
$2^3\Sigma_g^-$ - $1^5\Pi_g$
$2^3\Sigma_g^-$ - $3^5\Pi_g$
(C)
$E^3\Sigma_g^+$ - $3^3\Pi_g$
$E^3\Sigma_g^+$ - $2^3\Pi_g$
$E^3\Sigma_g^+$ - $B^3\Pi_g$
$E^3\Sigma_g^+$ - $1^3\Pi_g$
$E^3\Sigma_g^+$ - $2^5\Pi_g$
$E^3\Sigma_g^+$ - $3^5\Pi_g$
(D)

Figure 4

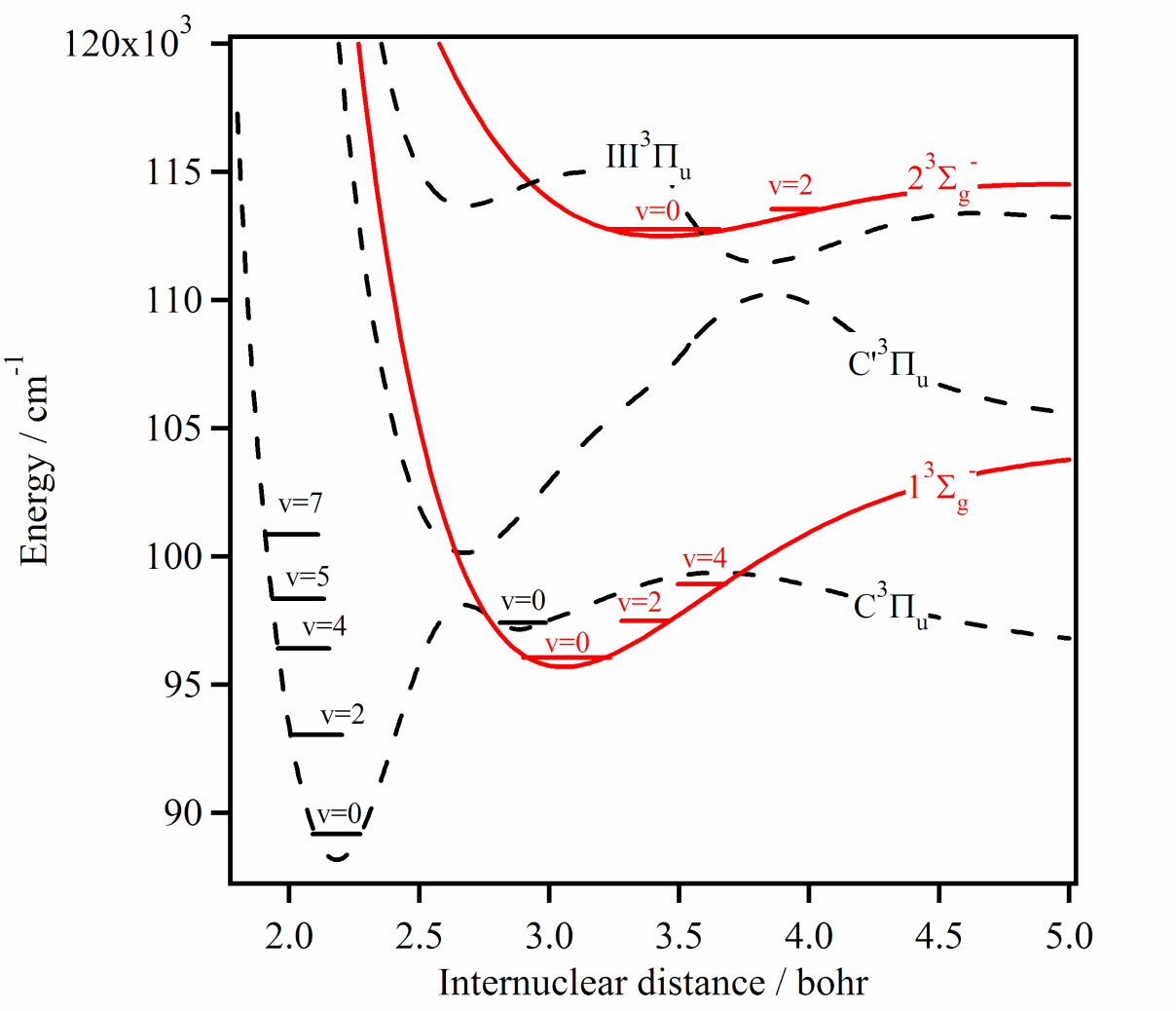
120x10^3
115
110
105
100
95
90
Energy / cm^-1
2.0
2.5
3.0
3.5
4.0
4.5
5.0
Internuclear distance / bohr
III^3Π_u
v=0
v=2
2^3Σ_g^-
C'^3Π_u
1^3Σ_g^-
v=4
C^3Π_u
v=0
v=2
v=0
v=7
v=5
v=4
v=2
v=0

Figure 5

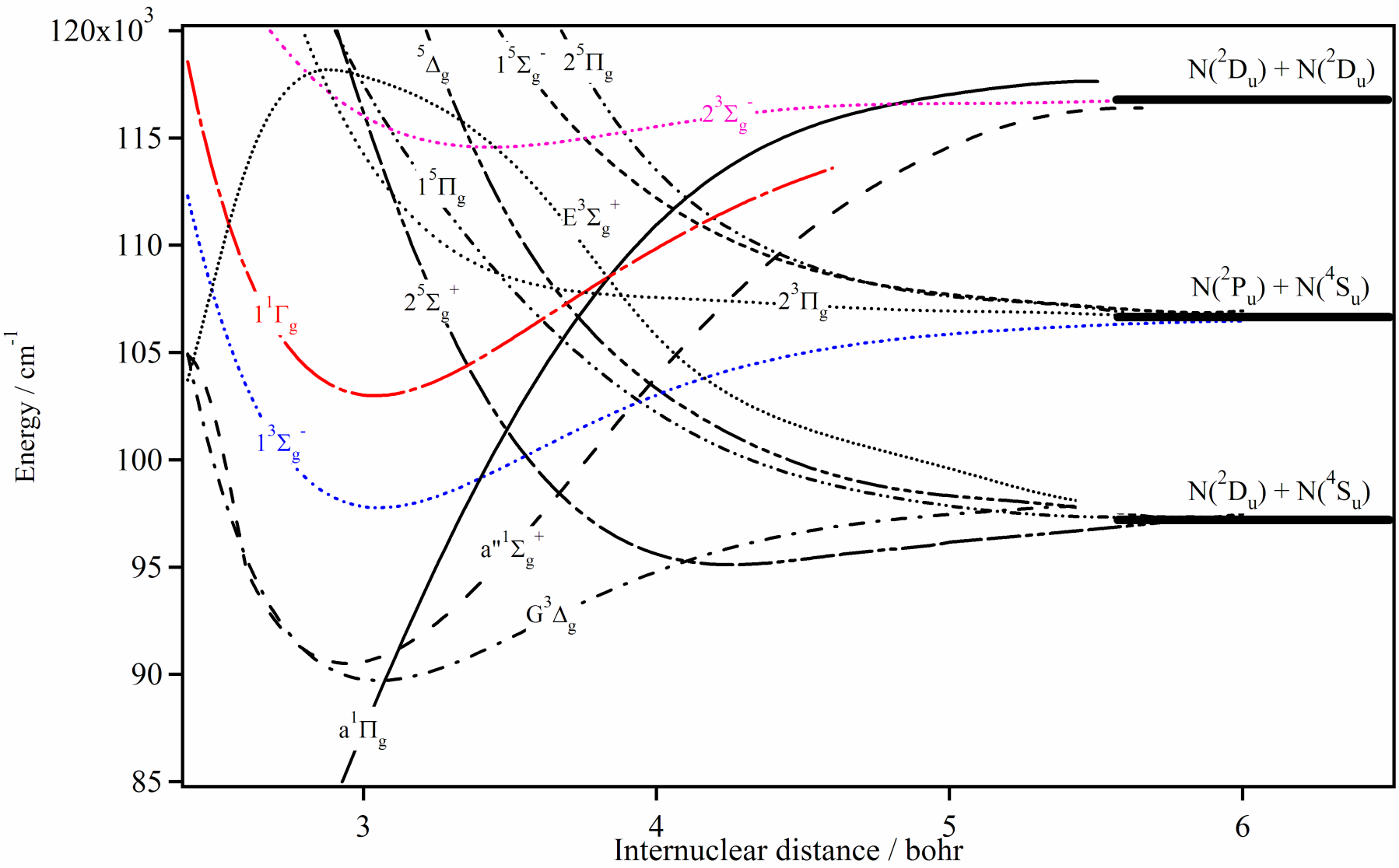
120x10^3
115
110
105
100
95
90
85
Energy / cm^-1
3
4
5
6
Internuclear distance / bohr
5Δg
1^5Σg^-
2^5Πg
2^3Σg^-
1^5Πg
E^3Σg^+
2^5Σg^+
2^3Πg
1^1Γg
1^3Σg^-
a''^1Σg^+
G^3Δg
a^1Πg
N(^2Du) + N(^2Du)
N(^2Pu) + N(^4Su)
N(^2Du) + N(^4Su)